PROCEEDINGS, Thirty-Eighth Workshop on Geothermal Reservoir Engineering
Stanford University, Stanford, California, February 11-13, 2013
SGP-TR-198

FREEZE-THAW-BEHAVIOUR: OBSERVATIONS IN GROUTED BHES

Hauke Anbergen and Ingo Sass

Technische Universität Darmstadt – Insitute of Applied Geoscience
Chair of Geothermal Science and Technology
D- 64287 Darmstadt, Germany
e-mail: anbergen@geo.tu-darmstadt.de

ABSTRACT

In Europe the construction of shallow geothermal heat-pump systems is expanding. The most favorable underground installation system is the borehole heat exchanger (BHE). Due to hydrogeological legal constraints, most BHEs have to be grouted and boreholes must remain sealed under all operating conditions. BHEs running with fluid temperatures below 0.0 °C (32.0 °F) are required to be sealed off with a grouting material that guarantees adequate sealing also under freeze-thaw-stresses. Even though requirements regarding the frost resistance of grouting material are laid down in the directives, there is no standardized and valid testing procedure to prove the required properties.

Therefore a testing device was invented (Fig. 1) that measures the hydraulic conductivity of grout specimens after a freely selectable number of cyclic freeze-thaw-stresses. Any pressure simulating radial earth pressure ($\sigma_2 = \sigma_3$) can be applied. The device is based on a triaxial flexible wall permeameter. Freezing direction is perpendicular to the BHE from the inside to the outside like in-situ. Results obtained with this set-up differ from earlier investigations substantially.

It was observed and modeled that the propagation of the frost front and the fabric disintegration processes are correlated. Numerical coupled modeling was applied to verify the results. More than 450 executed freeze-thaw-tests on different common grouting materials prove the characteristic influence of freezing-stresses on the hydraulic conductivity of grouted BHEs. As an outlook the implications for field practice will be supplied.

INTRODUCTION

Shallow geothermal systems can provide an efficient energy source to cover domestic heating and cooling demands. Especially for decentralized energy supply, ground coupled heat pump systems can be an alternative to common solely electrical heating/cooling or fossil fuels. Most ground coupled heat pumps in Europe are executed with BHEs.

For an optimized design of a BHE it is necessary to consider accurate parameters like thermal conductivity of the soils penetrated by the borehole. These parameters can be estimated using in-situ tests like the geothermal response test (GRT). Consequently the amount of thermal energy that can be supplied by the BHE can be calculated precisely and thus the whole system can be optimized.
An optimized system means that long-term sufficient temperature extraction is guaranteed. If the BHE is used monovalent for heating, it is likely that the soils temperature will decrease in the vicinity of the borehole, especially at the end of heating periods. In order to provide a sufficient heat extraction the heat pump will run with lower working fluid temperatures. To cover peak heating demands during that time, national directives (e.g. VDI, 2001) permit working fluid temperatures below 0.0 °C as negative peak temperatures. Thus freezing of the surrounding grout or even of surrounding soil cannot be ruled out.
An undersized borehole length or an increase in heating energy demand, which was not considered designing the specific system, may lead to even lower working fluid temperatures and at higher intervals. Hence freezing of the grout would become more likely.

It is obvious that freezing and thawing lead to different states of stress and consequently may lead to material disruptions. Due to some events of damage caused by frozen BHEs, authorities in central Europe became aware of this potential hazard. As a consequence some authorities do not permit working fluid temperatures below 0.0 °C anymore; some claim that grouting materials used for BHEs have to be frost-resistant. If peak working fluid temperatures below 0.0 °C are prohibited, the length of the BHEs must increase in order to cover the peak heating

demand, resulting in higher drilling and material costs.

Freezing and thawing stresses on soils, concrete, paper sludge or bentonite fillings have been evaluated widely so far. There exists a diversity of directives and standards for testing procedures and required material properties (e.g. ASTM D-6035-08, 2008). Unfortunately none exists specifically for grout materials for BHEs, neither in Europe, the U.S. or in any other country. There have been investigations on grouting materials, but the appliance of existing standards on grout is not trivial due to the specific boundary conditions of BHEs.

Testing Grout for BHEs

The grouting of BHEs has to meet two main requirements. On the one hand it has to seal off the borehole in order to prevent or minimize vertical water and mass flux. On the other hand it has to provide a sufficient heat flux towards the BHE (VDI, 2001). From a hydrogeological point of view the thermic requirement is of secondary priority; the proper sealing of eventual penetrated aquicludes is of prime importance. According to the presented specifications for grout testing, realistic statements are possible.

Parameters

Many methods exist to assess the influence of frost on material properties like compressive strength, volumetric change, acoustic impedance or hydraulic conductivity. In order to assess the susceptibility of the sealing effect of grouted BHEs, the hydraulic conductivity is chosen as the significant parameter. Hydraulic conductivity, based on the law of Darcy, is commonly used for geotechnical analysis and thus there exists a broad range of experiences in its implementation (CEN ISO/TS 17892-11:2004, ASTM Standard D5084-10). The presented hydraulic conductivity is calculated according to the European standard:

$$K = \frac{\Delta V \cdot L \cdot \alpha}{A \cdot \Delta h \cdot \Delta t} \quad (1)$$

where:

K = hydraulic conductivity, calculated to a temperature value of 10.0 °C (50.0 °F) (m s^{-1})
ΔV = quantity of water volume for given time interval Δt, flowing through specimen (m^{-3})
L = length of specimen (m)
A = cross-sectional area of specimen (m^2)
Δt = interval of time over which the flow of the water volume ΔV was measured (s)
α = transformation factor for temperature dependence of water viscosity
(CEN ISO/TS 17892-11:2004)

The K-Value is expressed for 10.0 °C a temperature corresponding to the average groundwater temperature in central Europe. The difference in viscosity between indoor temperature (about 20.0 °C/ 68.0 °F) and groundwater temperature (about 10.0 °C) induces a measured hydraulic conductivity that is approximately 30% higher than in situ.

Direction of freezing

Direction of freezing has a great influence on the location of ice lenses and thus on the location of the subsequent damage to the material. Frost heaving processes and ice lens growth have been widely analyzed (Konrad & Morgenstern, 1980, Ono, 2002, Coussy, 2005, Unold, 2006). The influence of frost on hydraulic conductivity has been quantified for paper sludge and benonites in several investigations and an ASTM Standard was established in 2008 (ASTM D-6035-08, 2008). Prior investigations on the freezing and thawing behavior of grouting materials have not considered the significant role of the direction of the heat flow. The frost front in BHEs primarily propagates radially from inside to the outside as the heat flow is directed (Carslaw & Jaeger, 1959, Sass & Lehr, 2011). Thus test specimens must also be frozen in this fashion. A freezing direction from the outside to the inside would lead to different results that do not reflect the in situ process.

Boundary conditions

During the freezing process ice lens growth may occur, inducing volumetric change. In-situ earth pressure hinders partly the volumetric expansion. A testing procedure without a confining radial cell-pressure would not reflect the geomechanical boundary conditions in a BHE. Thus expansion constraints have to be provided by an adequate testing procedure.

MATERIAL AND METHODS

Testing Device

The presented testing device is a modification of a triaxial flexible wall permeameter (Fig. 1). Specimens are fixed between an upper and a lower filter plate. These filter plates provide a homogeneous water flow for water permeability testing and prohibit an axial expansion induced by ice lens growth. Water pressure can be applied via the filter plates and connections to the laboratory equipment.

Cell pressure is applied between a membrane and a cylindrical rigid ring as abutment. Thus unplanned tangential water flow between the membrane and the lateral surface of the specimen is prevented. Furthermore a radial horizontal pressure can be applied, simulating earth pressure and thus allowing depth-dependent measurements. The fluid for the cell pressure is not in contact with the specimen itself. As the cell pressure must not vary during the freezing tests, the fluid is a mixture of water and glycol which provides sufficient frost protection and thus remains in a liquid state.

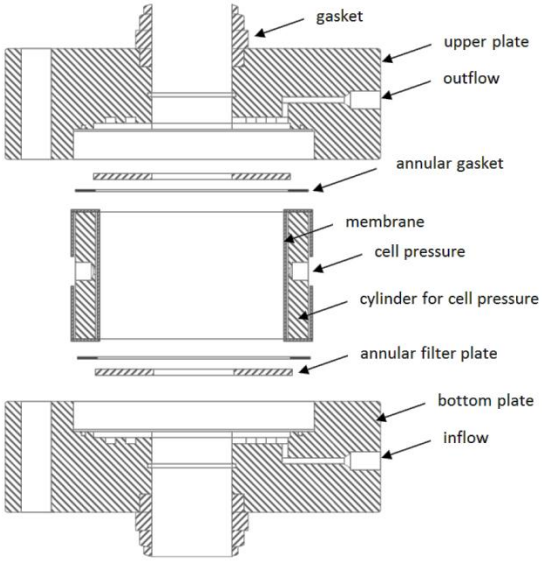

Figure 1: Schematic exploded drawing of the testing device.

Due to the special shape of the specimens gaskets are fitted in the upper and bottom plate. The gaskets prevent unwanted water flux. As the grouting material has to seal the BHE primarily in a vertical direction, the testing device measures the hydraulic conductivity along the axial direction of the specimen. Thus a statement about this most critical hydraulic path is feasible.
The testing device has approximately the same dimension as a regular triaxial permeability apparatus. Consequently the device can be implemented in any laboratory that possesses an apparatus for the determination of hydraulic conductivities of soils.

Specimens

As the specimens represent a slice of a BHE they are composed of a length of a pipe (simulating the probe) and the grout itself (Fig. 2). For consistent and standardized testing with comparable results, specimens have to be of exactly identical shape. In this case a perfectly axial embedment of the pipe into the surrounding grout body is realized.

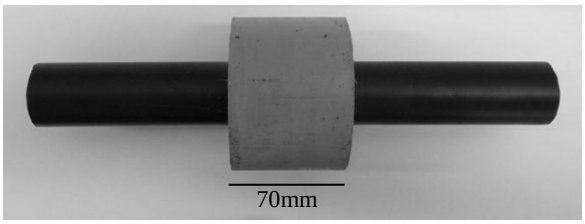

Figure 2: Specimen for freeze-thaw-testing.

This represents a simplified symmetrical geometry, the actual position of the probe in-situ will most likely vary from this idealized design. The contact surfaces and cross-sectional areas were calculated true to scale. Thus statements according to heat and water flow based on the investigation are feasible.
Therefore casting systems were constructed as presented in Fig. 3.

Figure 3: Casting systems.

The grout body of the specimen is trimmed in axial length to a cylindrical shape. Upper and lower cross-sectional area of the grout is enclosed tightly by the filter plates of the testing device during testing.

Testing Setup

After a defined setting time the grout specimen is transferred into the testing device. The testing device is closed up, gaskets are tightened and water pressure for saturation is applied according to the standards mentioned above (CEN ISO/TS 17892-11:2004, ASTM Standard D5084-10). Saturation is established and subsequently hydraulic conductivity is measured. For freeze-thaw-simulation saturation pressure is applied again in order to provide an unlimited water supply during the freezing process (Ono, 2002, Unold, 2006). The temperatures causing freezing and thawing are provided by a circular flow of working fluid through the pipe of the specimen. Working fluid temperature is controlled by a heat pump (Fig. 4). Specimens are allowed to freeze completely and then thaw again. Then hydraulic conductivity is measured.

Hence a potential change in hydraulic conductivity can be quantified.

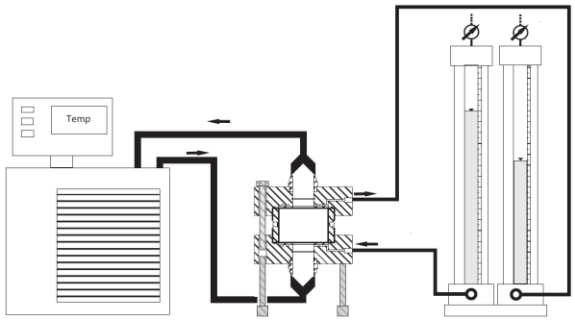

Figure 4: Schematic drawing of the testing setup.

Any number of freeze-thaw-cycles and measurements of hydraulic conductivity may be executed with the testing device. Performing one freeze-thaw-cycle including the subsequent determination of hydraulic conductivity takes 48 hours. The time demand was calculated with numerical simulations and temperature during every test is monitored. Thermocouples are mounted into the abutment cylinder measuring the temperature right next to the edge of the specimen and are connected to a data-logger. The testing device is insulated in order to reduce heat flux.

Numerical Model

The thermal process is modeled with the finite element modeling code FEFLOW. Since there are components of the testing device which are highly porous (filter plates and grout material) thermal hydraulic coupling is applied. Thus the hydraulic influence on the thermal distribution inside the modeled testing device is respected.
The coupled conductive and convective heat-transport is calculated according Eq. 2.

$$(\rho c)_g \frac{\partial T}{\partial t} = \nabla \cdot (\boldsymbol{\lambda} \nabla T - \rho_f c_f \mathbf{q} T) \qquad (2)$$

where:
$(\rho c)_g$ = bulk volumetric heat (J K^{-1} m^{-3})
T = temperature (°C)
λ = thermal conductivity tensor (W K^{-1} m^{-1})
ρ_f = density of fluid (
c_f = heat capacity of fluid (J g^{-1} K^{-1})
q = Darcy velocity (m s^{-1})
(Rühaak & Sass, 2013)

An excerpt of the assumed material properties is shown in Table 1.

Table 1: Thermal properties of the solid components of the modeled testing device (see Fig. 6).

Component	ε (-)	λ ($Wm^{-1}K^{-1}$)	c ($MJK^{-1}m^{-3}$)
Probe	1E-6	0.40	1.900
Grout	0.6	2.00	4.560
Filter plate	0.54	60.00	3.318
Upper and lower plate	1E-6	0.17	2.100
Membrane	1E-6	0.16	1.587
Insulation	1E-6	0.04	0.066

ε = porosity
λ = thermal conductivity of solid
c = volumetric heat

As the testing device is axisymmetric, the numerical model can be simplified (Fig. 5). The 2D sketch of the device is calculated as a rotationally symmetric body.

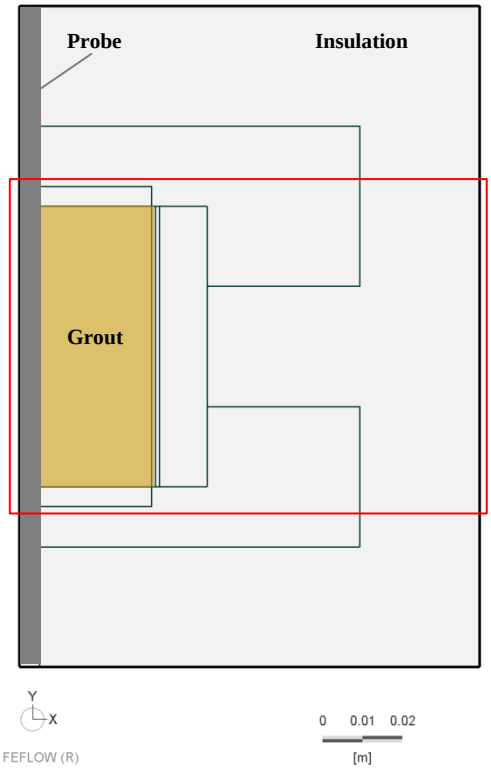

Figure 5: Location of the section (red) where the calculated temperature distribution is visualized in figures 8 through 11.

In Fig. 6 the thermal conductivities of the respective solid components of the model are visualized. The left-hand edge of the model represents the inner wall of the pipe. It is assumed that the temperature profile of the working fluid streaming through the pipe is constant along the axis. Thus a constant temperature

boundary condition is set during the freezing and thawing process.

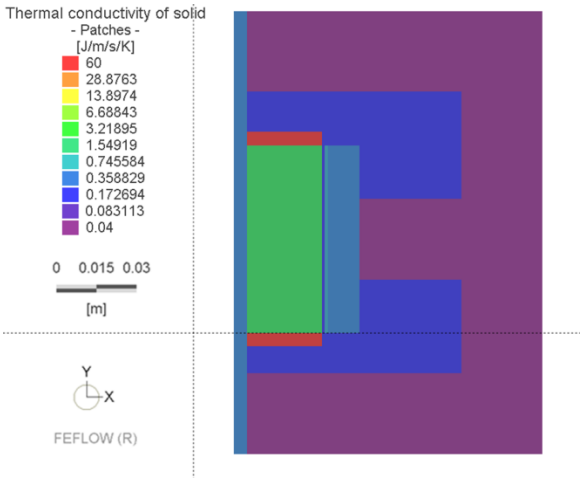

Figure 6: Thermal conductivity input parameters for the numerical FEFLOW-model.

The described numerical model allows predictions on the temperature distribution within the grout body of the specimens.

Thermographic Measurements

The freezing process in the grouted borehole of a BHE propagates radially and the testing procedure follows this freezing direction. As an experimental verification thermographic measurements were executed. Therefore specimens are subjected to the described testing procedure. After defined time intervals (one, four, five and fifteen hours) freezing is stopped, the testing device is opened, specimens are cut open and a thermography is taken. Thus temperature distribution on the split-area of the grout body is recorded and the propagation of the frost front can be comprehended. For each time interval a separate specimen is used.

RESULTS

Hydraulic Conductivity Test

The testing results of three different common grouting materials for BHEs are presented. Three specimens of each material were tested in order to verify the reproducibility of the results. Selected material properties are presented in Table 2.

Table 2: Relevant characteristics of the three tested grouting materials.

Grout	Thermally enhanced	Contains swelling clay minerals
Grout A	+	-
Grout B	+	+
Grout C	-	-

The hydraulic conductivities are measured before and after cyclic freeze-thaw-stress. The results of these tests are shown in Fig. 7.

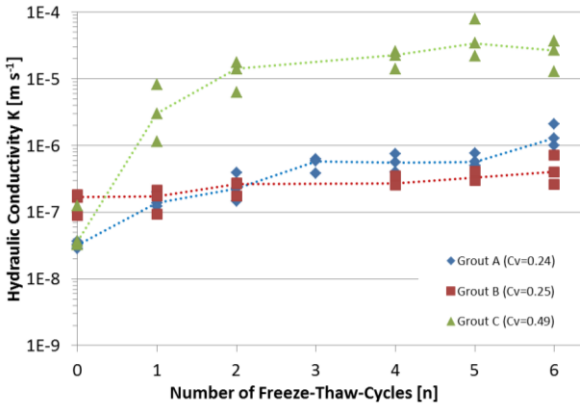

Figure 7: Hydraulic conductivity of specimens of three different grouting materials in dependence on the number of freeze-thaw-cycles. Dotted graph connects the median values.

The increase in hydraulic conductivity with increasing number of cyclic freeze-thaw-stresses is evident. This increase depends on the grouting material´s properties. Certain grouts have only a very low susceptibility to cyclic freeze-thaw-stresses (Grout B) and other materials are strongly influenced by the testing procedure (Grout C).
In Figure 7 the average weighted standard deviations (coefficient of variation C_V) of the measurement for each grout are listed. The C_Vs of Grout A and Grout B are of a value around 0.25. That underpins the characteristic behavior of the specimens during freeze-thaw-testing. Grout C has a relatively high C_V of 0.49. However it is noticeable that every specimen of the three tested shows an increase in hydraulic conductivity of two to three orders of magnitude.

Numerical Temperature Model

To visualize the temperature distribution inside the testing device, a section containing the grout body is chosen. The location of this section is outlined in Fig. 5 by the red box.
Fig. 8 to Fig. 11 each shows the temperature distributions at the respective time interval (one, four five and fifteen hours). Temperature isolines are given in degrees Celsius. After one hour of freezing (Fig. 8) the temperature inside the grout body has already decreased.

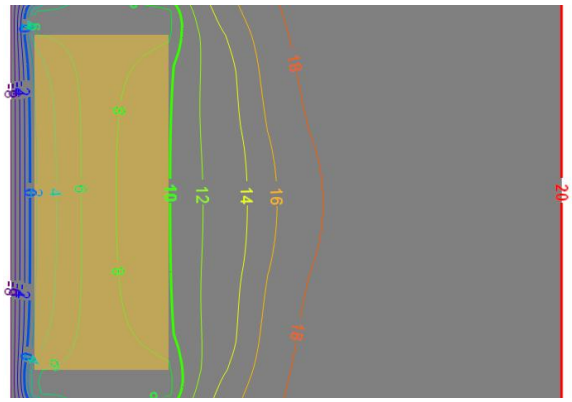

Figure 8: Temperature distribution (isolines) after one hour of freezing (FEFLOW). Grout specimen – dark-yellow; temperatures in degrees Celsius.

In Figure 9 the nearly vertical shape of the isoline of 0.0 °C is noticeable.

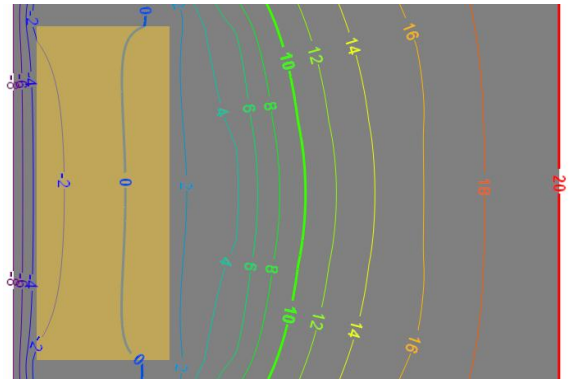

Figure 9: Temperature distribution (isolines) after four hours of freezing (FEFLOW). Grout specimen – dark-yellow; temperatures in degrees Celsius.

The radial distribution of the isolines can be observed (Fig. 9 and Fig. 10).

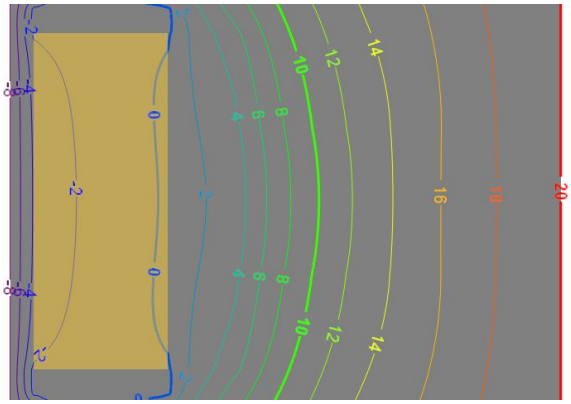

Figure 10: Temperature distribution (isolines) after five hours of freezing (FEFLOW). Grout specimen – dark-yellow; temperatures in degrees Celsius.

After fifteen hours of freezing (Fig.11) the temperature within the entire grout body has fallen below 0.0 °C.

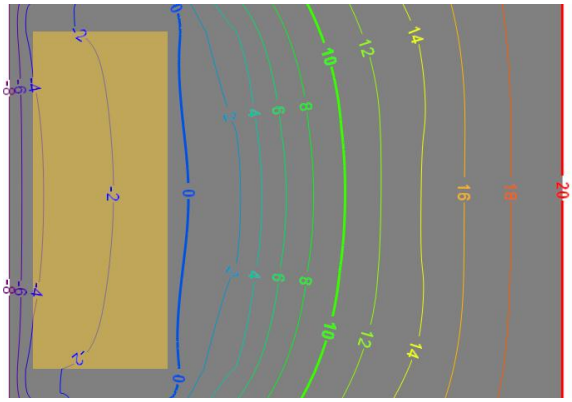

Figure 11: Temperature distribution (isolines) after fifteen hours of freezing (FEFLOW). Grout specimen – dark-yellow; temperatures in degrees Celsius.

The numerical solutions confirm the assumption that temperature propagation inside the specimens corresponds to the in-situ process in a grouted BHE.

Thermographic Measurements

The presented thermometry results (Fig. 13 – 16) are those of the identical time intervals as shown for the numerical results (Fig. 8 – 11). Specimens are fabricated of identical grouting material and under identical conditions (setting time, setting temperature etc.). As described the specimens are split up (Fig. 12) and the cross-section is measured with a thermography device. Due to the splitting process there are disturbances at the outer edge of the specimen (right-hand edge of Fig.12). Since the surface temperatures are measured, these disturbances have an influence on the results and need to be considered for the evaluation. The inner structure of the specimens is not thermally affected by the splitting process.

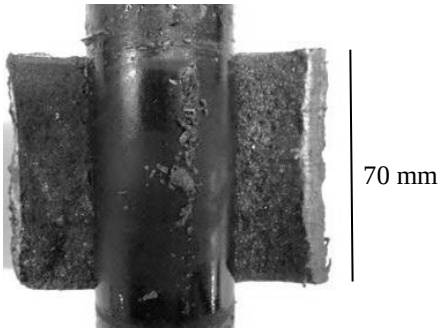

Figure 12: Photograph of a specimen prepared for thermography (split up).

After one hour of freezing (working fluid temperature of -10.0 °C/ +14.0 °F) the temperature of the grout body has decreased. Temperature at the inner edge of the grout body is lower than the temperature at the outer edge (Fig. 13).
The temperature scale is shown in the graphic and ranges from +15.0 °C (59.0 °F) to -9.0 °C (48.2 °F). Temperatures between 0.0 °C (32.0 °F) and -1.0 °C (30.2 °F) are colored grey.

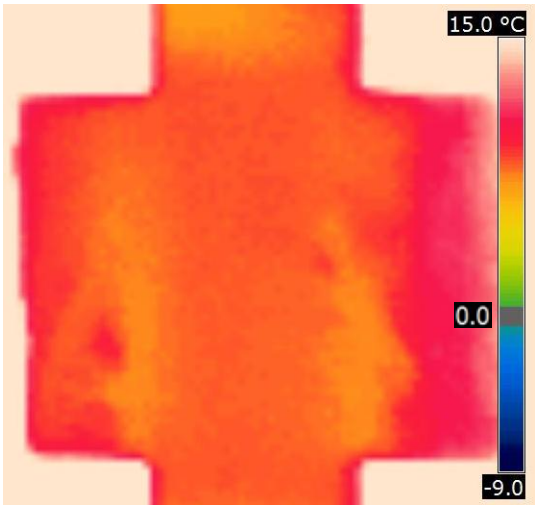

Figure 13: Thermography of a specimen (split up) after one hour of freezing.

Temperature inside the grout body decreases with increasing time of freezing. After a freezing period of four hours, the temperature has dropped below 0.0 °C. Again temperatures in the near field of the probe are the lowest (Fig. 14). The propagation of the frost front (respectively the isothermal curve of 0.0 °C where freezing can occur) moves radially from the inside to the outside.

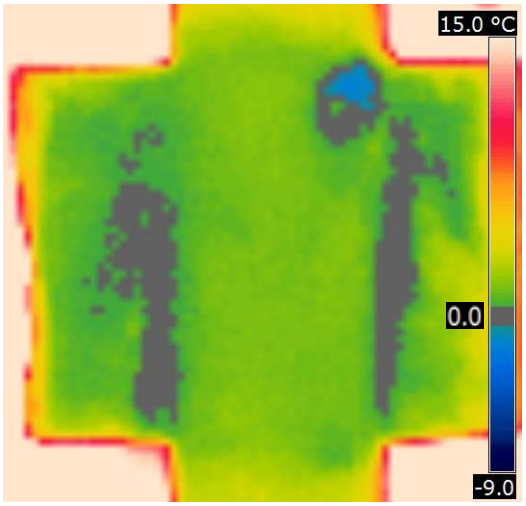

Figure 14: Thermography of a specimen (split up) after four hours of freezing.

With further increasing time temperature continues to decrease. The frost front moves radially from inside out. After five hours the temperature of nearly the whole specimen has dropped below 0.0 °C (Fig. 15).

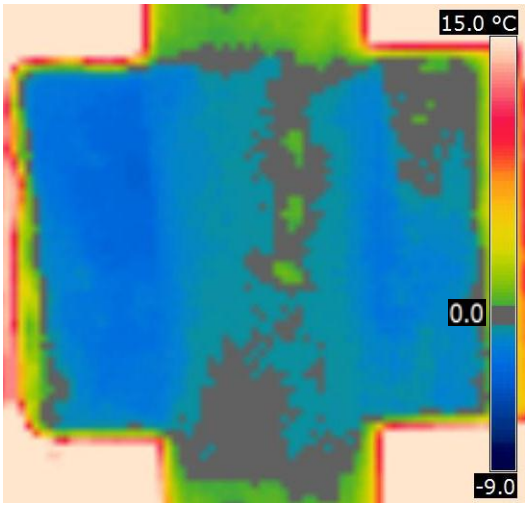

Figure 15: Thermography of a specimen (split up) after five hours of freezing.

It is noticeable that during the following freezing time, temperature of the whole specimen drops below 0.0 °C (Fig. 16) and remains in freezing temperature conditions until thawing is initialized.

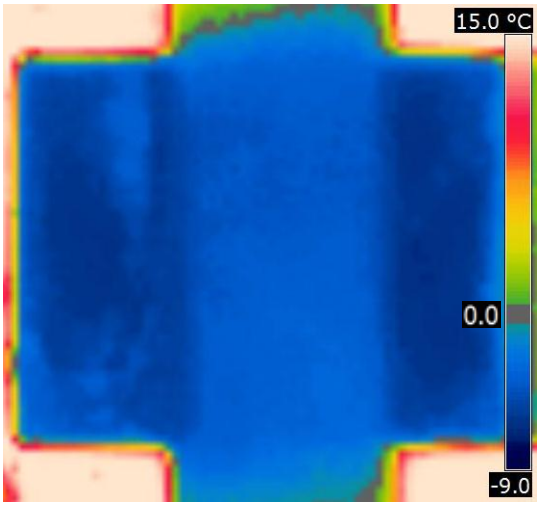

Figure 16: Thermography of a specimen (split up) after fifteen hours of freezing.

The thermographic measurements show that the freezing process inside the specimens corresponds to the radial shape of the freezing in BHEs. Since temperature is below 0.0 °C ice lens growth is possible.

Frost Induced Change in Structure

During the phase change of water and ice lens growth volumetric change occurs. This change exerts pressure that stresses the solid structure of the grout. It can be observed that the hypothesis of a radial heat flow and thus an axis-parallel frost front is confirmed. Frost induced disruptions in the specimens (Fig. 17) are mostly parallel and in axial direction. Cracking occurs in concentric circles. Specimens shown in Fig. 17 were subjected to six freeze-thaw-cycles. Grout A (left) and grout C (right) both show vertical cracks. The materials are marketed as resistant to cyclic freezing stresses and are frequently used for grouting BHEs. After testing, specimens were thoroughly dried at 105.0 °C (221.0 °F) removing all water from the specimen to prevent any effects of apparent cohesion.

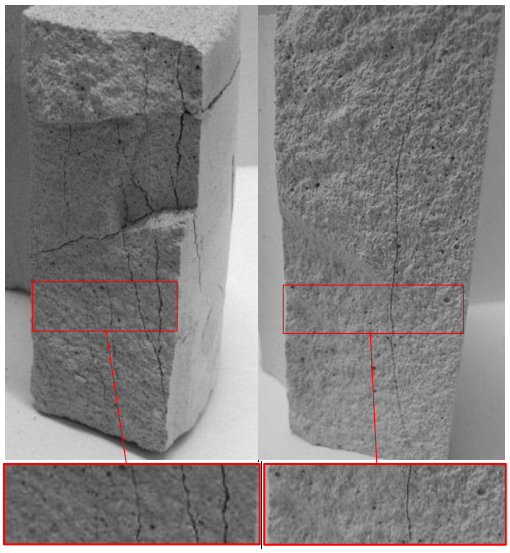

Figure 17: Frost induced cracks in specimens of Grout A (left) and Grout C (right) after six freeze-thaw-cycles and subsequent drying.

These cracks (Fig. 17) are preferred paths for water flux: However not every crack will inevitably increase the hydraulic conductivity of the specimen. Whether a crack has a great influence on the sealing effect or not, primarily depends on the content of swelling clays, e.g. bentonite. If a disruption occurs it is very likely that fine-grained components will swell, reduce the width of the crack and prevent unhindered water flux. Fig. 18 shows a specimen of another grouting material, that has no swelling clay components. The specimen was subjected to one freeze-thaw-cycle and subsequently dried.

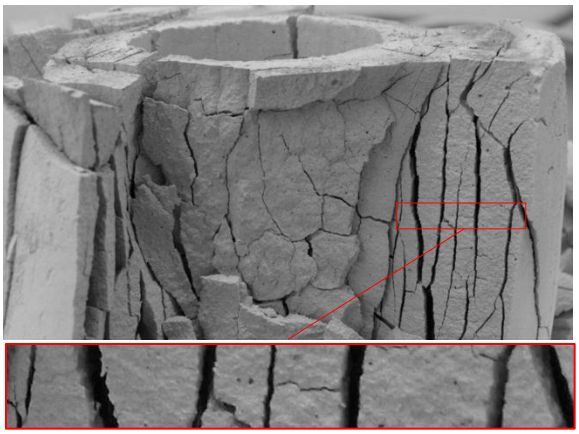

Figure 18: Frost induced cracks in specimen after one freeze-thaw-cycle and subsequent drying.

The disruptions are vertical as well. It is obvious the cracks appear perpendicular to the propagation of the frost front. Whether that tension stress causes cracking depends on the strength of the solid structure and the absolute value of superposing pressures. This can lead to cracks as mentioned above. However certain grouting materials are not susceptible to cyclic freeze-thaw-stresses. Fig. 19 shows a specimen of a grout cylinder without visible frost induced disruptions after six freeze-thaw-cycles.

Figure 19: Specimen of Grout B after six freeze-thaw-cycles and subsequent drying.

The specimens of Grout B display the lowest hydraulic conductivity after six freeze-thaw-cycles. This correlates with the visual observations of the cracking patterns (Fig.19).

DISCUSSION

The results of the numerical modeling correlate very well with the experimental observations. The propagation of the frost front is perpendicular to the axis of the specimen. The frost front moves radially from the inside to the outside.
Comparing the crack patterns of the specimens with the schematic process of ice lens growth in fine grained soils (Fig. 20), shows that these mechanisms correlate. During vertical frost penetration of soil a horizontal ice lens growth is observed (Konrad & Morgenstern, 1980).

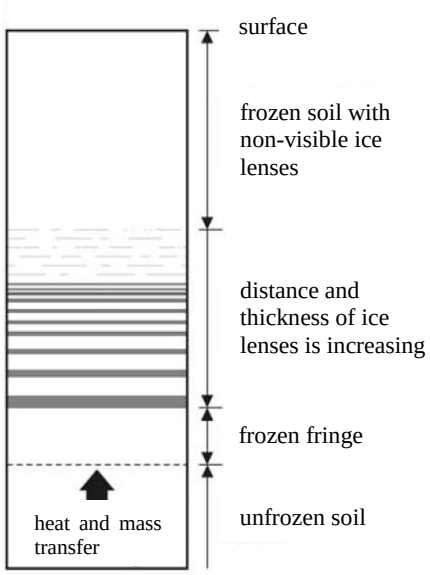

Figure 20: Schematic illustration of rhythmic ice lens formation in fine-grained soils. (Konrad & Morgenstern, 1980, Unold, 2006)

Ice lenses near the surface are of small diameter. The diameter increases with increasing distance to the location of frost penetration. This mechanism corresponds to the radial mechanism in the testing device (respective of BHE) and the crack pattern in Fig. 17.

CONCLUSION

The developed testing device and its setup produce feasible and reproducible results. The hydraulic conductivity of the three tested materials increases with cyclic freeze-thaw-stresses. The increase depends on the type of grouting material. Grout B shows the least increase in hydraulic conductivity and no visible frost induced cracks. This grouting material contains swelling clay minerals. The grouts without swelling clay components are more susceptible to cyclic freeze-thaw-stresses.

It is essential for a viable test procedure to freeze radially from the inside to the outside simulating the process of in-situ freezing. As frost induced cracks occur vertically in the direction of the most critical hydraulic pathway.

OUTLOOK

The testing device can be implemented easily in any geotechnical laboratory that possesses an apparatus for hydraulic conductivity testing. With its handling and high precision the procedure can contribute to quality assurance for shallow geothermal systems. Specimens can be prepared easily and freeze-thaw-test can be executed at reasonable expenses.
As the testing device and the whole procedure have proven its precision and practicability, further testing devices are being constructed and calibrated. Round robin tests in different European geotechnical laboratories will commence this spring. These tests will underpin the reproducibility and independency of the testing procedure. Thus the general conditions for a comprehensive quality assurance of frost-resistant grouting material will be provided.

The next step is to refine the numerical model through the implementation of phase changes, latent heat and crystallization effects into FEFLOW will be generated.

ACKNOWLEDGEMENTS

We would like to thank Jens Frank for his constant support and inspiring suggestions. Also we would like to thank Wolfram Rühaak for his suggestions to the numerical implementation and the State Ministry for Urban Development and the Environment Hamburg Germany for their help.

REFERENCES

ASTM Standard D5084-10 (2010), "Standard Test Methods for Measurement of Hydraulic Conductivity of Saturated Porous Materials Using a Flexible Wall Permeameter", Annual book of ASTM Standards, ASTM International, West Conshohocken, PA.

ASTM Standard D6035-08 (2008), "Standard Test Methods for Determing the Effect of Freeze-Thaw on Hydraulic Conductivity of Compacted or intact Soil Specimens Using a Flexible Wall Permeameter", Annual book of ASTM Standards, ASTM International, West Conshohocken, PA.

Carslaw, H.S. & Jaeger, J.C. (1959), "Conduction of Heat in Solids", Second Edition, Oxford University Press, Great Britain.

CEN ISO/TS 17892-11:2004 (2005), "Geotechnical investigation and testing Laboratory testing of soil Part 11: Determination of permeability by constant and falling head", Deutsches Institut für Normung, Beuth-Verlag, Berlin

Coussy, O. (2005), "Poromechanics of freezing materials", *Journal of the Mechanics and Physics of Solids*, **53**, 1689-1718

Konrad, J.-M. & Morgenstern, N.R. (1980), "A mechanistic theory of ice lens formation in fine-grained soils", *Canadian Geotechnical Journal*, **17**, 473-486.

Ono, T. (2002), "Lateral deformation of freezing clay under triaxial stress condition using laser-measuring device", *Cold Regions Science and Technology*, **35**, 45-54

Rühaak, W. & Sass, I. (2013), "Applied Thermo-Hydro-Mechanical coupled modeling of geothermal prospection in the northern Oberrheingraben", *Proceedings Thirty-Eighth Workshop on Geothermal Reservoir Engineering*, Stanford University, Stanford, CA

Sass, I. & Lehr, C. (2011), "Improvements on the Thermal Response Test Evaluation Applying the Cyclinder Source Therory", *Proceedings Thirty-Eighth Workshop on Geothermal Reservoir Engineering*, Stanford University, Stanford, CA

Unold, F. (2006), "Der Gefriersog bei der Durchfrostung und das Kompressionsverhalten des wieder aufgetauten Bodens", Ph.D. dissertation, Universität der Bundeswehr, München, Germany

VDI (ed.) (2001), "VDI-Guideline 4640 Part 2: Thermal use of the underground – Ground source heat pump systems", Beuth, Berlin.